ORGANOMETALLICS

pubs.acs.org/Organometallics Article

Thermal Dehydrogenation and Hydrolysis of BH_3NH_3 Catalyzed by Cyclic (Alkyl)(amino)carbene Iridium Complexes under Mild Conditions

Lei Zhou, Dejin Zhang, Jinling Hu, Youting Wu,* Jiao Geng,* and Xingbang Hu*

Cite This: *Organometallics* 2021, 40, 2643−2650

Read Online

ACCESS | Metrics & More | Article Recommendations | SI Supporting Information

ABSTRACT: Though ammonia−borane (AB) is recognized as an excellent hydrogen storage material, efficient dehydrogenation of AB still remains a challenge. Herein, we report that cyclic (alkyl)(amino)carbene iridium complexes are highly efficient for both the thermal dehydrogenation and hydrolysis of AB under mild conditions. At 30 °C, the two processes are completed within 15 and 5 min, releasing 2.1 and 2.8 equiv of H_2 per AB, respectively. Moreover, 2.8 equiv of H_2 can be released within 10 min by thermal dehydrogenation at 60 °C. Kinetic studies revealed that the activation energies for thermal dehydrogenation and hydrolysis of AB are 10.7 and 8.5 kcal/mol, respectively. The catalyst can be recycled without significant loss of activity at least six times for both processes. The reaction mechanisms were further explored by theoretical calculations, stoichiometric reactions, and kinetic isotope effect experiments.

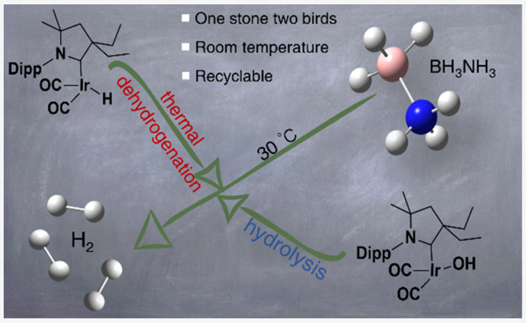

■ INTRODUCTION

Due to its high hydrogen content (19.6 wt %), nontoxicity, and stability at normal pressure and temperature,[1] ammonia−borane, $BH_3{\cdot}NH_3$ (AB), is regarded as an excellent chemical hydrogen-storage material.[2] Up to now, the dehydrogenation of AB has been studied extensively, through two different processes, namely hydrolysis[3] and thermal dehydrogenation.[4]

Rh@ZSM-5-H,[3g] Ni/Pt@ZIF-8,[3f] Rh/VO_2,[3e] and Ru/PC[3k] represent the most efficient catalysts for AB hydrolysis, since the process can be completed in a few minutes even at room temperature. In the case of thermal dehydrogenation, some catalysts afford linear polyaminoborane and 1 equiv of H_2, while others can generate >2 equiv of H_2 with concomitant formation of a cyclic iminoborane trimer (borazine) and its BN-cross-linked oligomers (polyborazylene).[5] Thermal dehydrogenation of AB is more difficult, and only a fraction of the hydrogen can be released in hours even at high temperatures.[4a−d,f−j] For example, AB thermal dehydrogenation catalyzed by sterically encumbered pyridones releases only 1.9 equiv of H_2 at 80 °C in 2 h.[4j] Using Fe pincer complexes, 2.5 equiv of H_2 is released at 60 °C, but after 15 h.[4g] When graphene oxide was used as the catalyst, the reaction required 100 °C to release 2.3 equiv of H_2 in 8 h.[6] It is quite clear that, due to the difference in mechanisms for AB thermal dehydrogenation and hydrolysis, the catalysts reported for these two processes are quite different.

Cyclic (alkyl)(amino)carbenes (CAACs),[7] in which one of the electron π-donating and σ-withdrawing electronegative amino substituents of NHCs is replaced by a σ-donor alkyl group, are more nucleophilic (σ-donating) but also more electrophilic (π-accepting) than NHCs.[8] These electronic properties give them the ability to activate a variety of bonds and small molecules[9] and to stabilize highly reactive main-group and transition-metal diamagnetic and paramagnetic species.[10] CAACs can be used as very robust catalysts for a variety of applications.[11] Manners and co-workers used different CAACs as hydrogen acceptors to study the dehydropolymerization of phosphine−borane.[12]

Bertrand et al. and we have already reported that CAAC copper complexes are active in AB hydrolysis,[3d] but we found that they have no activity for the thermal dehydrogenation process. Herein, we show that CAAC iridium complexes efficiently promote both the hydrolysis and thermal dehydrogenation of AB under mild conditions. More than 2.7 equiv of H_2 can be released in both processes. Moreover, mechanisms for the hydrolysis and thermal dehydrogenation reactions are proposed.

Received: May 20, 2021
Published: July 19, 2021

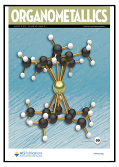

https://doi.org/10.1021/acs.organomet.1c00302
Organometallics 2021, 40, 2643−2650

■ RESULTS AND DISCUSSION

Synthesis of Complexes 1a–c and 2a–c. Two CAACs (CAAC^{Et2} and CAAC^{Cy}) and one NHC were prepared from the corresponding conjugate acids **a**–**c** according to reported procedures.[7a] Then, $[\text{Ir(cod)Cl}]_2$ was reacted with these carbenes to give (CAAC^{Et2})Ir(cod)Cl (**1a**), (CAAC^{Cy})Ir(cod)Cl (**1b**), and (NHC)Ir(cod)Cl (**1c**) (Scheme 1).

Scheme 1. Synthetic Toute of CAAC/NHC-Ir Complexes 1a–c and 2a–c and X-ray Structure of 1b (CCDC-2023438)[a]

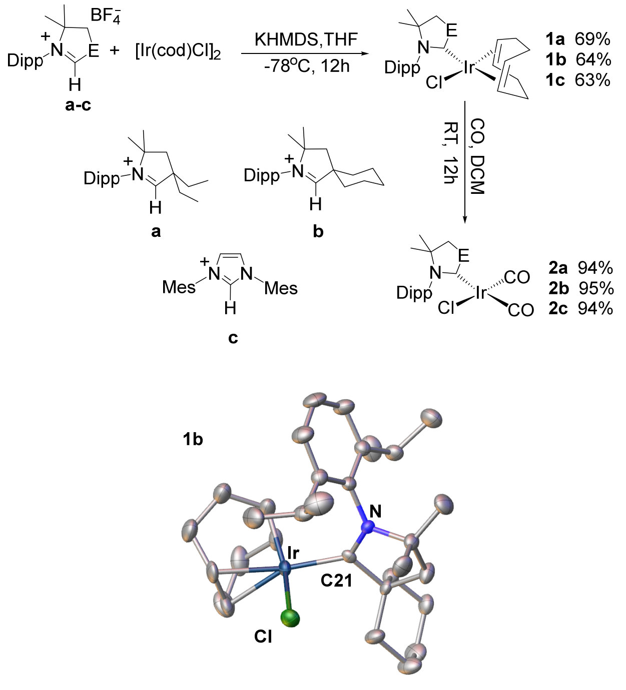

[a] Hydrogen atoms are omitted for clarity. Selected bond lengths (Å) and angles (deg): Ir–Cl 2.3977(17), Ir–C21 2.012(6), N–C21 1.327(7), Ir–C21–N 128.8(4).

Crystals of **1b** suitable for a single-crystal X-ray diffraction analysis were obtained in ethyl ether solution. Subsequent carbonylation[13] was carried out to produce (CAAC^{Et2})Ir$(\text{CO})_2$Cl (**2a**), (CAAC^{Cy})Ir$(\text{CO})_2$Cl (**2b**), and (NHC)Ir$(\text{CO})_2$Cl (**2c**). All of these complexes are stable in air for months.

Thermal Dehydrogenation of AB. (CAAC)Ir complexes **1a**,**b** (5 mol %) were first tested for the AB thermal dehydrogenation, and after 2 h at 60 °C, 2.2 and 2.5 equiv of H_2, respectively, were released (Figure 1). Carbonyl complexes **2a**,**b** were even more efficient, with 2.8 and 2.7 equiv of H_2 released, under the same experimental conditions. Interestingly, only 1.5 equiv of H_2 was released with **2c**, featuring an NHC ligand. The superior efficiency of (CAAC)Ir complexes, over their NHC counterparts, is probably due to their better σ-donating and π-accepting properties.[7a,c,8c,14] Although potassium *tert*-butoxide itself has no catalytic activity for the dehydrogenation, we found that addition of KO^{t}Bu greatly accelerates the reaction: 2.8 and 2.1 equiv of H_2 were obtained within 10 and 15 min at 60 and 30 °C, respectively (Figure 2). This combination represents the most active catalytic system for the thermal dehydrogenation of AB reported to date (the TOF value is up to 2880 $\text{mol}_{\text{H2}}\ \text{mol}_{\text{cat}}^{-1}\ \text{h}^{-1}$ at 30 °C; see Table S1).

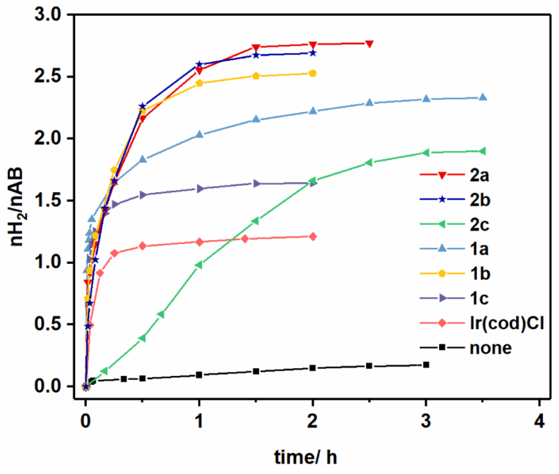

Figure 1. Thermal dehydrogenation of AB (15 mg) at 60 °C with different catalysts (5 mol %). Solvent: 0.5 mL of dried THF and 2 mL of dried diglyme.

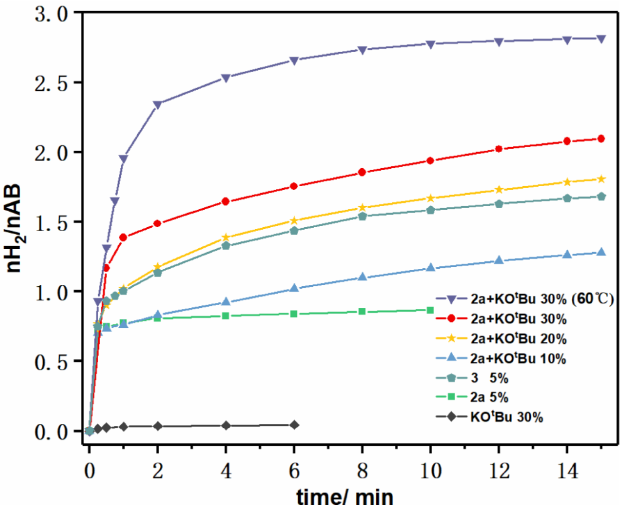

Figure 2. Thermal dehydrogenation of AB (15 mg) at 30 °C using **2a** (5 mol %) with different amounts of KO^{t}Bu. Solvent: 0.5 mL of dried THF and 2 mL of dried diglyme.

The products of AB thermal dehydrogenation were characterized by ^{11}B NMR (Figure 3) and FT-IR (Figure S39). On comparison with the literature,[4f,g,5b] the thermal dehydrogenation products were confirmed to be cyclotriborazane (CTB), borazine, and polyborazylene (PB), and no polyaminoborane was observed.[5a,15]

Hydrolysis of AB. In addition to the thermal dehydrogenation, **2a** also serves as a highly effective catalyst for the AB hydrolysis, and KO^{t}Bu also facilitates this process (Figure 4). It is worth noting that KO^{t}Bu had no catalytic activity, but it can be used as an effective additive. On the one hand, it might increase the pH value of the reaction system, which is beneficial for AB dehydrogenation (Figure S29). On the other hand, it is possible that deactivation of the catalyst is decreased under the more basic conditions, as alkoxides could protect the active sites.[3i,16] At 30 °C, 2.8 equiv of H_2 was obtained within 5 min in the presence of **2a** and KO^{t}Bu. Moreover, nearly 3.0 equiv of H_2 was obtained within 2 min at 45 °C. On the basis

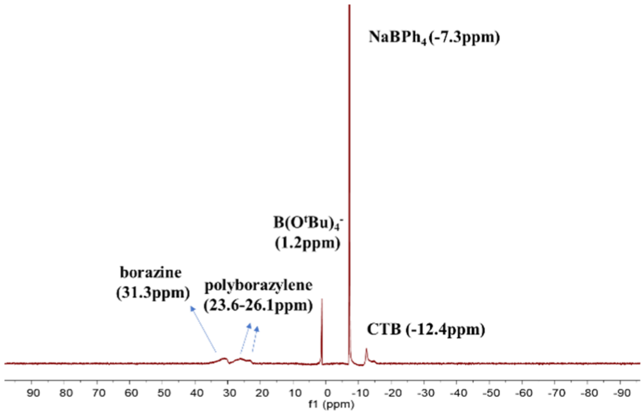

Figure 3. ^{11}B NMR spectrum of AB thermal dehydrogenation, with $NaBPh_4$ as an internal standard in THF, locked by a C_6D_6 capillary insert. Reaction conditions: **2a** 5% + KO^{t}Bu 30%, 30 °C, 20 min.

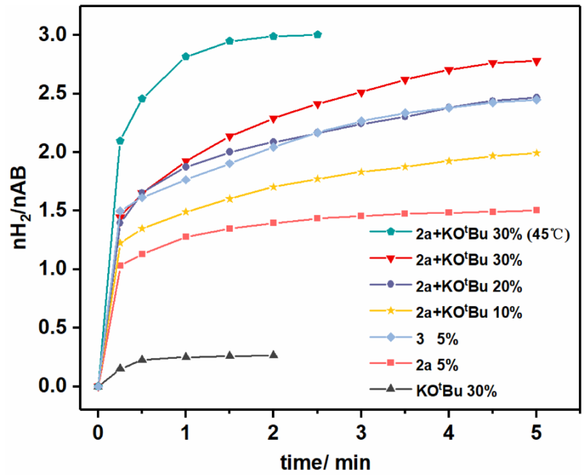

Figure 4. Hydrolysis of AB (15 mg) at 30 °C using **2a** (5 mol %) with different amounts of KO^{t}Bu. Solvent: 0.5 mL of dried THF and 2 mL of deionized water.

of ^{11}B NMR (Figure 5) and FT-IR (Figure S39), the AB hydrolysis products were confirmed to be borates.[3c−l]

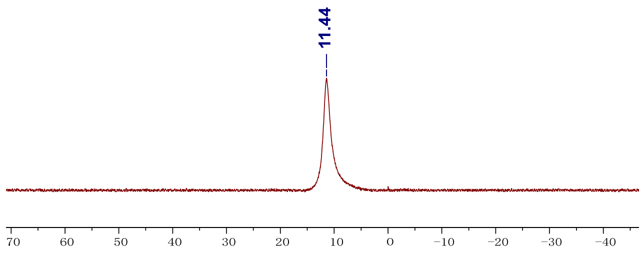

Figure 5. ^{11}B NMR spectra of the product of AB hydrolysis (locked by D_2O).

Figure 6 displays the effect of AB concentration on the AB hydrolysis with **2a** as the catalyst; with an increase in AB concentration, the amount of H_2 released increased.[17] The influence of different **2a** loadings on the H_2 generation rate was investigated. As shown in Figure 7, the AB hydrolysis rate increased continuously with increasing catalyst loading.[18]

Recycling of Catalysts in AB Thermal Dehydrogenation and Hydrolysis. The recycling of a catalyst is one of the most important aspects for practical applications.[3g] The results of AB thermal dehydrogenation and hydrolysis recycling processes are shown in Figure 8. For each cycle, the thermal dehydrogenation and hydrolysis reactions were finished within 15 and 5 min, and the releases of H_2 were about 2.1 and 2.8 equiv, respectively. The mixture of 5% **2a** and 30% KO^{t}Bu was reused six times without any noticeable loss of catalytic activity.

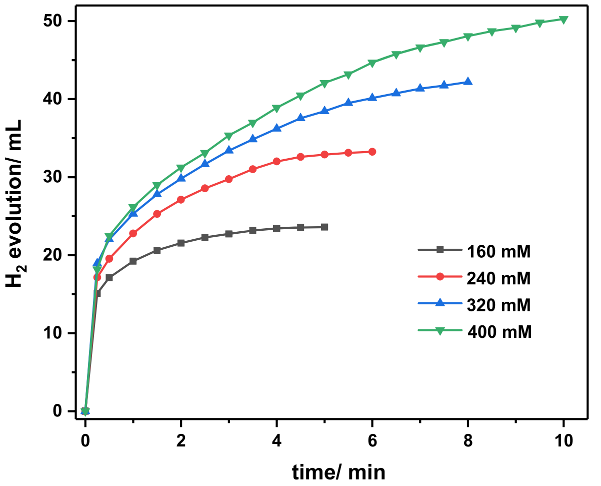

Figure 6. Time dependence of hydrogen evolution versus time with different concentrations of AB on AB hydrolysis at 30 °C, with 5 mol % of **2a** as catalyst. Solvent: 0.5 mL of dried THF and 2 mL of deionized water. Portions of 12.3, 18.5, 24.6, and 30.8 mg of AB were added to prepare solutions with different concentrations of AB.

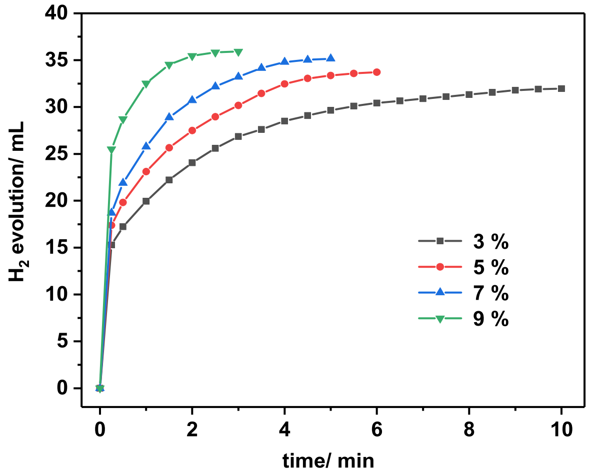

Figure 7. Time dependence of hydrogen evolution versus time with different concentrations of **2a** on AB hydrolysis at 30 °C. Solvent: 0.5 mL of dried THF and 2 mL of deionized water.

Mechanisms for AB Thermal Dehydrogenation and Hydrolysis. To understand the high efficiency of (CAAC)Ir complexes for the AB dehydrogenation, a stoichiometric reaction between **2a** and AB was performed (Scheme 2). In addition to a signal at −10.1 ppm due to the formation of the two Ir−H−B groups, a signal for Ir−H was found in the ^1H NMR at −13.3 ppm (Figure S43), suggesting that the reaction may produce the oxidative addition product of B−H bonds to the CAAC-Ir complex $(CAAC)IrH(BH_2ClNH_3)(CO)_2$ (**4**).[19] The resonance at −8.4 ppm in ^{11}B NMR spectra (Figure S34) indicates the existence of $BH_2Cl{\cdot}NH_3$.[4i] Indeed, theoretical calculations revealed that the Gibbs free energy change from

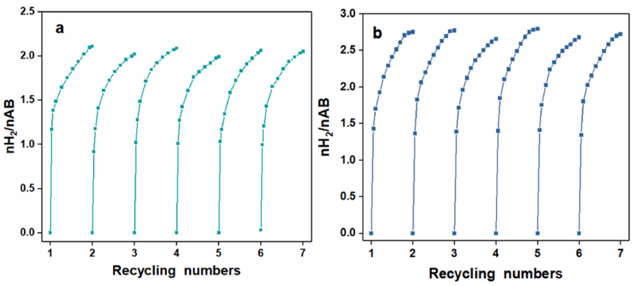

Figure 8. (a) Recycling of catalyst in the AB thermal dehydrogenation at 30 °C (5% **2a** + 30% KO^{t}Bu). Reaction time for each cycle: 15 min. Solvent: 0.5 mL of dried THF and 2 mL of dried diglyme. (b) Recycling of catalyst in the AB hydrolysis at 30 °C (5% **2a** + 30% KO^{t}Bu). Reaction time for each cycle: 5 min. Solvent: 0.5 mL of dried THF and 2 mL of deionized water.

Scheme 2. Plausible Path for the Stoichiometric Reaction between 2a and AB[a]

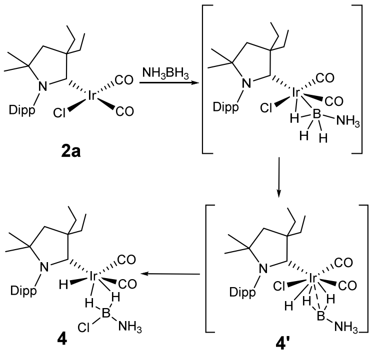

[a]The Gibbs free energy change from **4′** to **4** is −20.1 kcal/mol.

(CAAC)IrHCl(BH$_2$NH$_3$)(CO)$_2$ **4′** to **4** was −20.1 kcal/mol. On the other hand, we found that **2a** reacts with potassium *tert*-butoxide to give (CAAC)Ir(CO)$_2$O^{t}Bu (**3**), which appeared to be highly reactive with water, affording (CAAC)-Ir(CO)$_2$OH (**5**), even at room temperature. The energy barrier for this reaction was calculated to be only 7.4 kcal/mol, and the Gibbs free energy change was −1.7 kcal/mol (Figure S41). Hence, we hypothesize that (CAAC)IrH(BH$_2$ClNH$_3$)-(CO)$_2$ (**4**) and (CAAC)IrOH(CO)$_2$ (**5**) are the active intermediates in the thermal dehydrogenation and hydrolysis, respectively (Scheme 3), and calculations were performed (see the Supporting Information for the details of calculation methods).

For the thermal dehydrogenation catalyzed by CAAC-Ir, the reactive speciation **4-IrH** can be released by **4** with a small Gibbs free energy change (3.7 kcal/mol) (Figure 9a). Because the hydrogen of Ir−H carried a negative charge (−0.101), the formation of H$_2$ between **4-IrH** and BH$_3$·NH$_3$ is quite easy via the transition state **TS1$_{py}$**. In **TS1$_{py}$**, the Ir−H bond length increases from 1.665 to 1.837 Å, and the H−H distance is 0.848 Å. Following **TS1$_{py}$**, a (CAAC)IrNH$_2$BH$_3$(CO)$_2$ intermediate is formed. A hydride transfer from H−B of NH$_2$BH$_3$ to the Ir center via **TS2$_{py}$** regenerates **4-IrH**. The energy barrier for the rate-determining step of the thermal dehydrogenation is only 14.7 kcal/mol (**TS1$_{py}$**), which is significantly lower than those reported using 6-*tert*-butyl-2-thiopyridone (26.8 kcal/mol),[4j] a nickel N-heterocyclic carbene (25.1 kcal/mol),[20] an Ir dihydrogen pincer complex (18.1 kcal/mol),[4b] and Ir-(PCy$_3$)$_2$(H)$_2$ (21.3 kcal/mol)[21] as catalysts. A similar process catalyzed by NHC-Ir has also been investigated (Figure 9b). In comparison with CAAC-Ir, NHC-Ir gives a higher energy barrier for the rate-determining step (18.2 vs 14.7 kcal/mol). This agrees well with the experimental result,s which show that CAAC-Ir is more reactive (Figure 1).

Scheme 3. Proposed Dehydrogenation Mechanism for AB Thermal Dehydrogenation and Hydrolysis Catalyzed by CAAC-Ir Complexes

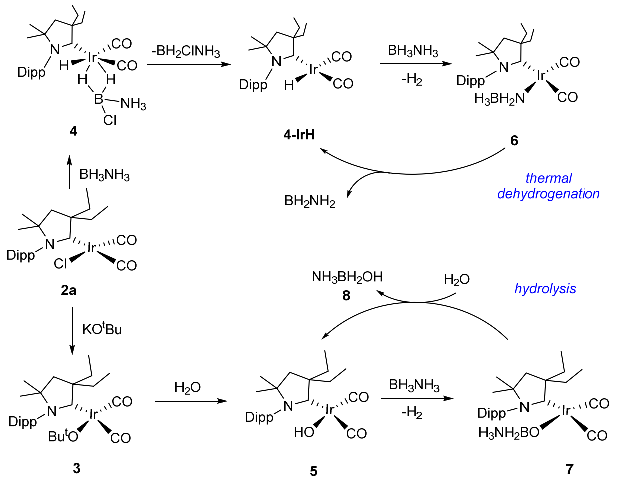

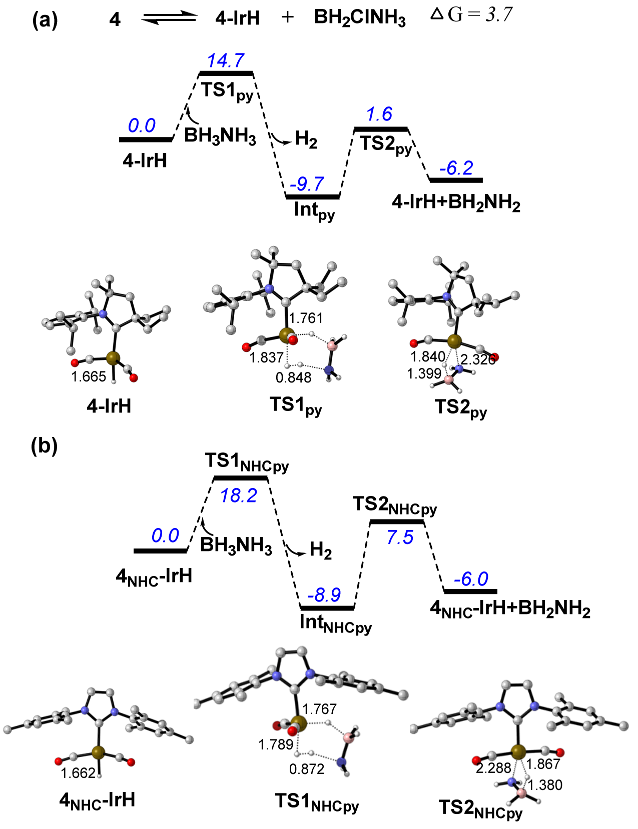

Figure 9. Energy profile and optimized structures for the thermal dehydrogenation catalyzed by (a) (CAAC)Ir and (b) (NHC)Ir complexes. The values in italics are the energies in kcal/mol, and other values are the bond distances in Å.

For the hydrolysis, the formation of H$_2$ occurs between the proton of Ir−OH and H−B via the transition state **TS1$_{hy}$** (Figure 10). In **TS1$_{hy}$**, the O−H bond length increases from

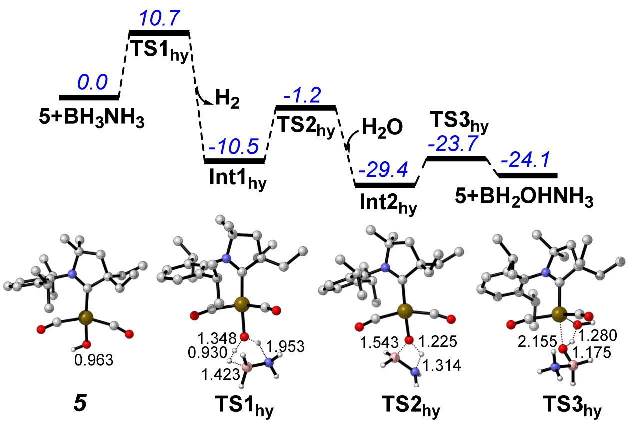

Figure 10. Energy profile and optimized structures for the hydrolysis catalyzed by (CAAC)Ir complexes. The values in italics are energies in kcal/mol, and other values are bond distances in Å.

0.963 to 1.348 Å, and the H−H distance is 0.930 Å. (CAAC)Ir(CO)$_2$OBH$_2$NH$_3$ is formed as an intermediate. Being similar to (CAAC)Ir(CO)$_2$O^{t}Bu (**3**), CAAC-Ir-OBH$_2$NH$_3$ is sensitive to H$_2$O. Hydrolysis of (CAAC)Ir(CO)$_2$OBH$_2$NH$_3$ via **TS3$_{hy}$** (barrier: 5.7 kcal/mol) regenerates (CAAC)Ir(CO)$_2$OH (**5**). The energy barrier for the rate-determining step is only 10.7 kcal/mol (**TS1$_{hy}$**), which is lower than those of other catalysts, such as [Cp*Ir(6,6′-(OH)$_2$-bpy)(OH$_2$)]SO$_4$ (24.2 kcal/mol) and Ru-(p-Cym)(bipy) (15.1 kcal/mol).[22]

Since (CAAC)IrH(BH$_2$ClNH$_3$)(CO)$_2$ (**4**) and (CAAC)-IrOH(CO)$_2$ (**5**) are the postulated active intermediates for the thermal dehydrogenation and hydrolysis, their formation is crucial for the dehydrogenation process. It is interesting to find that the rate of Ir−H formation in the presence of KO^{t}Bu is faster than that without KO^{t}Bu (Figure 11). This agrees well with the thermal dehydrogenation results (Figure 2), confirming that the Ir−H compound is the active intermediate in the thermal dehydrogenation. On the other hand, previous reports revealed that the reaction between (CAAC)AuO^{t}Bu and water to produce (CAAC)Au−OH is almost 144 times faster than the ion exchange between (CAAC)AuCl and KOH.[23] Replacing the KO^{t}Bu with KOH in the hydrolysis of AB resulted in a slower dehydrogenation rate (Figure S42), further supporting that (CAAC)Ir(CO)$_2$OH (**5**) is the active intermediate in this process.

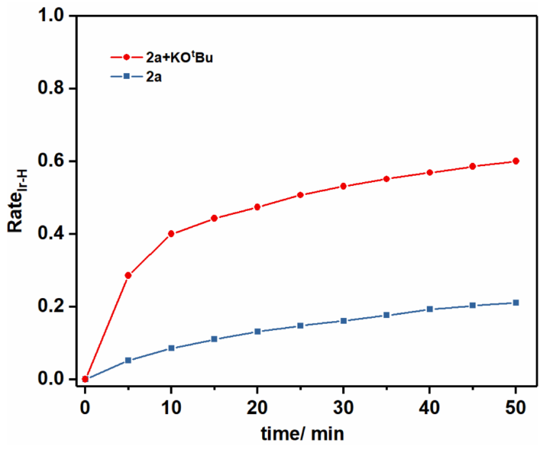

Figure 11. Rate of Ir−H formation between **2a** and AB with and without KO^{t}Bu. The reaction took place in a nuclear magnetic tube at RT. Rate$_{Ir-H}$ = n(Ir−H)/n(**2a**) determined by ^{1}H NMR (see Figure S41).

In addition, a series of deuterated amine−boranes have been prepared.[4c,24] As illustrated in Figure 12, deuteration of AB on either the nitrogen or the boron site results in a slower rate. The result of the individual KIEs (kinetic isotope effects) $(k_{NH_3\cdot BH_3}/k_{NH_3\cdot BD_3}) \times (k_{NH_3\cdot BH_3}/k_{ND_3\cdot BH_3}) = 1.64 \times 1.86 = 3.05$ is similar to the KIE observed for the doubly labeled substrate $(k_{NH_3\cdot BH_3}/k_{ND_3\cdot BD_3} = 2.80)$. This reveals that both B−H and N−H bonds are broken in the rate-determining step,[4g−i] which agrees well with the theoretical calculation results.

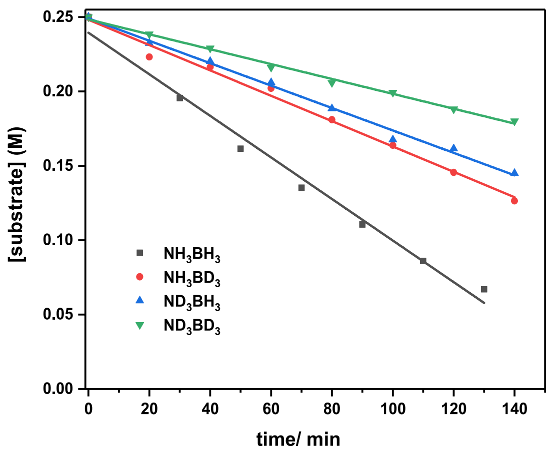

Figure 12. Consumption of NH$_3$·BH$_3$ and its isotopomers (0.25 M in 1/4 THF/diglyme 2.5 mL) in the presence of 5 mol % of **2a** at RT.

Further experiments were performed in order to confirm the fate of the reaction between Ir−H and Ir−OH and BH$_3$·NH$_3$. To avoid the uncontrollable reaction of BH$_3$·NH$_3$, BEt$_3$·NH$_3$ was used to react with Ir−H and the dehydrogenation product **6′** was characterized by mass spectroscopy but was not isolable (Scheme 4). Similarly, ammonia−9-borabicyclo[3.3.1]nonane (BH(C$_8$H$_{14}$)NH$_3$) was used to react with (CAAC)Ir-(CO)$_2$OH (**5**) and the dehydrogenation product **7′** was observed, again only by mass spectroscopy.

Scheme 4. Further Evidence for the Involvement of Ir−H and Ir−OH Complexes in the AB Thermal Dehydrogenation and Hydrolysis

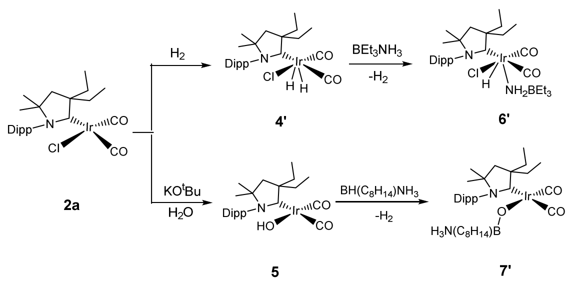

Finally, to further verify the computational results, kinetic studies of AB thermal dehydrogenation and hydrolysis were performed. The dehydrogenation reactions of AB catalyzed by **2a** were carried out at different temperatures, and the results are shown in Figure 13. They suggest that both thermal

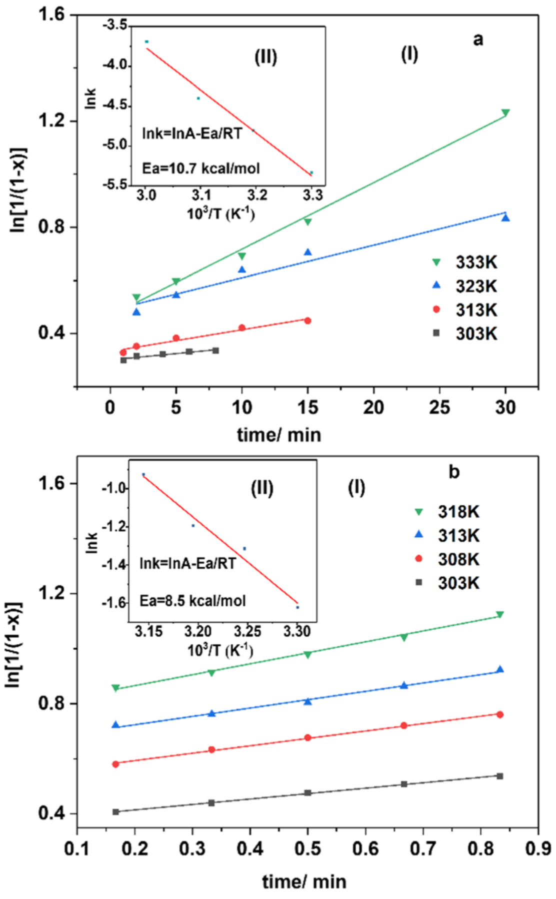

Figure 13. (a) (I) Effect of the temperature on the thermal dehydrogenation rate of AB with 5 mol % of **2a**. (II) Arrhenius plots of the rate constant of AB thermal dehydrogenation. (b) (I) Effect of the temperature on the hydrolysis rate of AB with 5 mol % of **2a**. (II) Arrhenius plots of the rate constant of AB hydrolysis.

dehydrogenation and hydrolysis of AB are first-order reactions,[25] with activation energies of 10.7 and 8.5 kcal/mol, respectively. These experimental results are in agreement with the theoretical data, considering the systematic error of both experiment and theoretical calculations. They show that the energy barrier for the hydrolysis is lower than that for the thermal dehydrogenation.

■ CONCLUSIONS

Under mild conditions, a mixture of CAAC^{Et2}-Ir$(CO)_2$Cl and KO^{t}Bu promotes the hydrolysis and thermal dehydrogenation of AB. These processes are completed within 5 and 15 min, and 2.8 and 2.1 equiv of H_2 per AB, respectively, are released. Moreover, 2.8 equiv of H_2 can be released in less than 10 min by AB thermal dehydrogenation at 60 °C. The catalytic solution can be handled in air and recycled without a significant loss of activity. Experiments combined with theoretical calculations revealed that (CAAC)Ir$(CO)_2$H and (CAAC)Ir$(CO)_2$OH are most likely the active intermediates for the thermal dehydrogenation and hydrolysis, respectively. From kinetics experiments, the activation energies of the AB thermal dehydrogenation and hydrolysis were found to be 10.7 and 8.5 kcal/mol, respectively.

For the first time, a single catalyst is reported to be highly effective for both the hydrolysis and thermal dehydrogenation of AB, and CAAC-Ir complexes represent the most active catalysts reported so far for the thermal dehydrogenation.

■ ASSOCIATED CONTENT

Supporting Information

The Supporting Information is available free of charge at https://pubs.acs.org/doi/10.1021/acs.organomet.1c00302.

Experimental details, original spectra, X-ray diffraction tables, and theoretical calculation details (PDF)

Cartesian coordinates of the optimized structures (MOL)

Accession Codes

CCDC 2023438 contains the supplementary crystallographic data for this paper. These data can be obtained free of charge via www.ccdc.cam.ac.uk/data_request/cif, or by emailing data_request@ccdc.cam.ac.uk, or by contacting The Cambridge Crystallographic Data Centre, 12 Union Road, Cambridge CB2 1EZ, UK; fax: +44 1223 336033.

■ AUTHOR INFORMATION

Corresponding Authors

Youting Wu − *School of Chemistry and Chemical Engineering, Nanjing University, Nanjing 210093, People's Republic of China*; Email: ytwu@nju.edu.cn

Jiao Geng − *School of Chemistry and Chemical Engineering, Nanjing University, Nanjing 210093, People's Republic of China*; Email: gengjiao@nju.edu.cn

Xingbang Hu − *School of Chemistry and Chemical Engineering, Nanjing University, Nanjing 210093, People's Republic of China*; orcid.org/0000-0002-2995-9704; Email: huxb@nju.edu.cn

Authors

Lei Zhou − *School of Chemistry and Chemical Engineering, Nanjing University, Nanjing 210093, People's Republic of China*

Dejin Zhang − *School of Chemistry and Chemical Engineering, Nanjing University, Nanjing 210093, People's Republic of China*

Jinling Hu − *School of Chemistry and Chemical Engineering, Nanjing University, Nanjing 210093, People's Republic of China*

Complete contact information is available at: https://pubs.acs.org/10.1021/acs.organomet.1c00302

Notes

The authors declare no competing financial interest.

■ ACKNOWLEDGMENTS

We thank Prof. Guy Bertrand for valuable suggestions and discussions. This work was supported by the National Natural Science Foundation of China (Nos. 21878141 and 22078145) and the Key Research & Development Plan of Jiangsu Province (BE2019095).

■ REFERENCES

(1) (a) Kumar, R.; Karkamkar, A.; Bowden, M.; Autrey, T. Solid-State Hydrogen Rich Boron-Nitrogen Compounds for Energy Storage. *Chem. Soc. Rev.* **2019**, *48*, 5350−5380. (b) Wang, Q.; Fu, F.; Yang, S.; Martinez, M. M.; Moya, S.; Salmon, L.; Ruiz, J.; Astruc, D. Dramatic Synergy in CoPt Nanocatalysts Stabilized by "Click"

Dendrimers for Evolution of Hydrogen from Hydrolysis of Ammonia Borane. *ACS Catal.* **2019**, *9*, 1110−1119.

(2) (a) Rossin, A.; Peruzzini, M. Ammonia-Borane and Amine-Borane Dehydrogenation Mediated by Complex Metal Hydrides. *Chem. Rev.* **2016**, *116*, 8848−8872. (b) Han, D. L.; Anke, F.; Trose, M.; Beweries, T. Recent Advances in Transition Metal Catalysed Dehydropolymerisation of Amine Boranes and Phosphine Boranes. *Coord. Chem. Rev.* **2019**, *380*, 260−286.

(3) (a) Fortman, G. C.; Slawin, A. M. Z.; Nolan, S. P. Highly Active Iridium(III)-NHC System for the Catalytic B-N Bond Activation and Subsequent Solvolysis of Ammonia-Borane. *Organometallics* **2011**, *30*, 5487−5492. (b) Li, P.; Aijaz, A.; Xu, Q. Highly Dispersed Surfactant-Free Nickel Nanoparticles and Their Remarkable Catalytic Activity in the Hydrolysis of Ammonia Borane for Hydrogen Generation. *Angew. Chem., Int. Ed.* **2012**, *51*, 6753−6756. (c) Chen, W.; Ji, J.; Feng, X.; Duan, X.; Qian, G.; Li, P.; Zhou, X.; Chen, D.; Yuan, W. Mechanistic Insight into Size-Dependent Activity and Durability in Pt/Cnt Catalyzed Hydrolytic Dehydrogenation of Ammonia Borane. *J. Am. Chem. Soc.* **2014**, *136*, 16736−16739. (d) Hu, X.; Soleilhavoup, M.; Melaimi, M.; Chu, J.; Bertrand, G. Air-Stable (CAAC)CuCl and (CAAC)CuBH$_4$ Complexes as Catalysts for the Hydrolytic Dehydrogenation of BH$_3$NH$_3$. *Angew. Chem., Int. Ed.* **2015**, *54*, 6008−6011. (e) Wang, L.; Li, H.; Zhang, W.; Zhao, X.; Qiu, J.; Li, A.; Zheng, X.; Hu, Z.; Si, R.; Zeng, J. Supported Rhodium Catalysts for Ammonia-Borane Hydrolysis: Dependence of the Catalytic Activity on the Highest Occupied State of the Single Rhodium Atoms. *Angew. Chem., Int. Ed.* **2017**, *56*, 4712−4718. (f) Fu, F.; Wang, C.; Wang, Q.; Martinez-Villacorta, A. M.; Escobar, A.; Chong, H.; Wang, X.; Moya, S.; Salmon, L.; Fouquet, E.; Ruiz, J.; Astruc, D. Highly Selective and Sharp Volcano-Type Synergistic Ni$_2$Pt@ZIF-8-Catalyzed Hydrogen Evolution from Ammonia Borane Hydrolysis. *J. Am. Chem. Soc.* **2018**, *140*, 10034−10042. (g) Sun, Q.; Wang, N.; Zhang, T.; Bai, R.; Mayoral, A.; Zhang, P.; Zhang, Q.; Terasaki, O.; Yu, J. Zeolite-Encaged Single-Atom Rhodium Catalysts: Highly-Efficient Hydrogen Generation and Shape-Selective Tandem Hydrogenation of Nitroarenes. *Angew. Chem., Int. Ed.* **2019**, *58*, 18570−18576. (h) Li, H.; Yan, Y.; Feng, S.; Zhu, Y.; Chen, Y.; Fan, H.; Zhang, L. Novel Method of High-Efficient Synergistic Catalyze Ammonia Borane Hydrolysis to Hydrogen Evolution and Catalytic Mechanism Investigation. *Fuel* **2019**, *255*, 115771. (i) Qu, X.; Jiang, R.; Li, Q.; Zeng, F.; Zheng, X.; Xu, Z.; Chen, C.; Peng, J. The Hydrolysis of Ammonia Borane Catalyzed by NiCoP/Opc-300 Nanocatalysts: High Selectivity and Efficiency, and Mechanism. *Green Chem.* **2019**, *21*, 850−860. (j) Wang, H.; Gao, C.; Li, R.; Peng, Z.; Yang, J.; Gao, J.; Yang, Y.; Li, S.; Li, B.; Liu, Z. Ruthenium-Cobalt Nanoalloy Embedded within Hollow Carbon Spheres as a Bifunctionally Robust Catalyst for Hydrogen Generation from Water Splitting and Ammonia Borane Hydrolysis. ACS Sustain. *ACS Sustainable Chem. Eng.* **2019**, *7*, 18744−18752. (k) Ding, R.; Chen, Q.; Luo, Q.; Zhou, L.; Wang, Y.; Zhang, Y.; Fan, G. Salt Template-Assisted in Situ Construction of Ru Nanoclusters and Porous Carbon: Excellent Catalysts toward Hydrogen Evolution, Ammonia-Borane Hydrolysis, and 4-Nitrophenol Reduction. *Green Chem.* **2020**, *22*, 835−842. (l) Wang, Y.; Shen, G.; Zhang, Y.; Pan, L.; Zhang, X.; Zou, J. Visible-Light-Induced Unbalanced Charge on NiCoP/TiO$_2$ Sensitized System for Rapid H$_2$ Generation from Hydrolysis of Ammonia Borane. *Appl. Catal., B* **2020**, *260*, 118183. (m) Liu, S.; Li, Y.; Zheng, X.; Guan, X.; Zhang, X.; Liu, P. Pd Nanoparticles Anchoring to Core-Shell Fe$_3$O$_4$@SiO$_2$-Porous Carbon Catalysts for Ammonia Borane Hydrolysis. *Int. J. Hydrogen Energy* **2020**, *45*, 1671−1680.

(4) (a) Denney, M. C.; Pons, V.; Hebden, T. J.; Heinekey, D. M.; Goldberg, K. I. Efficient Catalysis of Ammonia Borane Dehydrogenation. *J. Am. Chem. Soc.* **2006**, *128*, 12048−12049. (b) Paul, A.; Musgrave, C. B. Catalyzed Dehydrogenation of Ammonia-Borane by Iridium Dihydrogen Pincer Complex Differs from Ethane Dehydrogenation. *Angew. Chem., Int. Ed.* **2007**, *46*, 8153−8156. (c) Keaton, R. J.; Blacquiere, J. M.; Baker, R. T. Base Metal Catalyzed Dehydrogenation of Ammonia-Borane for Chemical Hydrogen Storage. *J. Am. Chem. Soc.* **2007**, *129*, 1844−1845. (d) Hebden, T. J.; Denney, M. C.; Pons, V.; Piccoli, P. M. B.; Koetzle, T. F.; Schultz, A. J.; Kaminsky, W.; Goldberg, K. I.; Heinekey, D. M. Sigma-Borane Complexes of Iridium: Synthesis and Structural Characterization. *J. Am. Chem. Soc.* **2008**, *130*, 10812−10820. (e) Staubitz, A.; Sloan, M. E.; Robertson, A. P. M.; Friedrich, A.; Schneider, S.; Gates, P. J.; Schmedt auf der Gunne, J.; Manners, I. Catalytic Dehydrocoupling/Dehydrogenation of N-Methylamine-Borane and Ammonia-Borane: Synthesis and Characterization of High Molecular Weight Polyaminoboranes. *J. Am. Chem. Soc.* **2010**, *132*, 13332−13345. (f) Staubitz, A.; Robertson, A. P. M.; Manners, I. Ammonia-Borane and Related Compounds as Dihydrogen Sources. *Chem. Rev.* **2010**, *110*, 4079−4124. (g) Bhattacharya, P.; Krause, J. A.; Guan, H. Mechanistic Studies of Ammonia Borane Dehydrogenation Catalyzed by Iron Pincer Complexes. *J. Am. Chem. Soc.* **2014**, *136*, 11153−11161. (h) Glueer, A.; Foerster, M.; Celinski, V. R.; auf der Guenne, J. S.; Holthausen, M. C.; Schneidert, S. Highly Active Iron Catalyst for Ammonia Borane Dehydrocoupling at Room Temperature. *ACS Catal.* **2015**, *5*, 7214−7217. (i) Lu, Z.; Schweighauser, L.; Hausmann, H.; Wegner, H. A. Metal-Free Ammonia-Borane Dehydrogenation Catalyzed by a Bis(Borane) Lewis Acid. *Angew. Chem., Int. Ed.* **2015**, *54*, 15556−15559. (j) Hasenbeck, M.; Becker, J.; Gellrich, U. Efficient Organocatalytic Dehydrogenation of Ammonia Borane. *Angew. Chem., Int. Ed.* **2020**, *59*, 1590−1594.

(5) (a) Staubitz, A.; Presa Soto, A.; Manners, I. Iridium-Catalyzed Dehydrocoupling of Primary Amine-Borane Adducts: A Route to High Molecular Weight Polyaminoboranes, Boron-Nitrogen Analogues of Polyolefins. *Angew. Chem., Int. Ed.* **2008**, *47*, 6212−6215. (b) Kalviri, H. A.; Gartner, F.; Ye, G.; Korobkov, I.; Baker, R. T. Probing the Second Dehydrogenation Step in Ammonia-Borane Dehydrocoupling: Characterization and Reactivity of the Key Intermediate, B-(Cyclotriborazanyl)Amine-Borane. *Chem. Sci.* **2015**, *6*, 618−624. (c) Johnson, H. C.; Hooper, T. N.; Weller, A. S. The Catalytic Dehydrocoupling of Amine−Boranes and Phosphine−Boranes. *Top. Organomet. Chem.* **2015**, *49*, 153.

(6) Tang, Z.; Chen, H.; Chen, X.; Wu, L.; Yu, X. Graphene Oxide Based Recyclable Dehydrogenation of Ammonia Borane within a Hybrid Nanostructure. *J. Am. Chem. Soc.* **2012**, *134*, 5464−5467.

(7) (a) Lavallo, V.; Canac, Y.; Prasang, C.; Donnadieu, B.; Bertrand, G. Stable Cyclic (Alkyl)(Amino)Carbenes as Rigid or Flexible, Bulky, Electron-Rich Ligands for Transition-Metal Catalysts: A Quaternary Carbon Atom Makes the Difference. *Angew. Chem., Int. Ed.* **2005**, *44*, 5705−5709. (b) Soleilhavoup, M.; Bertrand, G. Cyclic (Alkyl)-(Amino)Carbenes (CAACs): Stable Carbenes on the Rise. *Acc. Chem. Res.* **2015**, *48*, 256−266. (c) Melaimi, M.; Jazzar, R.; Soleilhavoup, M.; Bertrand, G. Cyclic (Alkyl)(Amino)Carbenes (CAACs): Recent Developments. *Angew. Chem., Int. Ed.* **2017**, *56*, 10046−10068. (d) Paul, U. S. D.; Radius, U. What Wanzlick Did Not Dare to Dream: Cyclic (Alkyl)(Amino)Carbenes (CAACs) as New Key Players in Transition-Metal Chemistry. *Eur. J. Inorg. Chem.* **2017**, *2017*, 3362−3375.

(8) (a) Lavallo, V.; Canac, Y.; Donnadieu, B.; Schoeller, W. W.; Bertrand, G. Co Fixation to Stable Acyclic and Cyclic Alkyl Amino Carbenes: Stable Amino Ketenes with a Small Homo-Lumo Gap. *Angew. Chem., Int. Ed.* **2006**, *45*, 3488−3491. (b) Droege, T.; Glorius, F. The Measure of All Rings-N-Heterocyclic Carbenes. *Angew. Chem., Int. Ed.* **2010**, *49*, 6940−6952. (c) Hopkinson, M. N.; Richter, C.; Schedler, M.; Glorius, F. An Overview of N-Heterocyclic Carbenes. *Nature* **2014**, *510*, 485−496. (d) Vatsadze, S. Z.; Loginova, Y. D.; Dos Passos Gomes, G.; Alabugin, I. V. Stereoelectronic Chameleons: The Donor−Acceptor Dichotomy of Functional Groups. *Chem. - Eur. J.* **2017**, *23*, 3225−3245.

(9) (a) Frey, G. D.; Lavallo, V.; Donnadieu, B.; Schoeller, W. W.; Bertrand, G. Facile Splitting of Hydrogen and Ammonia by Nucleophilic Activation at a Single Carbon Center. *Science* **2007**, *316*, 439−441. (b) Frey, G. D.; Masuda, J. D.; Donnadieu, B.; Bertrand, G. Activation of Si-H, B-H, and P-H Bonds at a Single Nonmetal Center. *Angew. Chem., Int. Ed.* **2010**, *49*, 9444−9447. (c) Martin, D.; Soleilhavoup, M.; Bertrand, G. Stable Singlet Carbenes as Mimics for Transition Metal Centers. *Chem. Sci.* **2011**,

2, 389−399. (d) Wurtemberger-Pietsch, S.; Schneider, H.; Marder, T. B.; Radius, U. Adduct Formation, B−H Activation and Ring Expansion at Room Temperature from Reactions of HBcat with NHCs. *Chem. - Eur. J.* **2016**, *22*, 13032−13036. (e) Mohapatra, C.; Samuel, P. P.; Li, B.; Niepotter, B.; Schurmann, C. J.; Herbst-Irmer, R.; Stalke, D.; Maity, B.; Koley, D.; Roesky, H. W. Insertion of Cyclic Alkyl(Amino) Carbene into the Si−H Bonds of Hydrochlorosilanes. *Inorg. Chem.* **2016**, *55*, 1953−1955. (f) Zhukhovitskiy, A. V.; Mavros, M. G.; Queeney, K. T.; Wu, T.; Van Voorhis, T.; Johnson, J. A. Reactions of Persistent Carbenes with Hydrogen-Terminated Silicon Surfaces. *J. Am. Chem. Soc.* **2016**, *138*, 8639−8652. (g) Pietrasiak, E.; Lee, E. Activation of C-F, Si-F, and S-F Bonds by N-Heterocyclic Carbenes and Their Isoelectronic Analogues. *Synlett* **2020**, *31*, 1349−1360. (h) Peltier, J. L.; Tomas-Mendivil, E.; Tolentino, D. R.; Hansmann, M. M.; Jazzar, R.; Bertrand, G. Realizing Metal-Free Carbene-Catalyzed Carbonylation Reactions with Co. *J. Am. Chem. Soc.* **2020**, *142*, 18336−18340.

(10) (a) Martin, C. D.; Soleilhavoup, M.; Bertrand, G. Carbene-Stabilized Main Group Radicals and Radical Ions. *Chem. Sci.* **2013**, *4*, 3020−3030. (b) Martin, D.; Moore, C. E.; Rheingold, A. L.; Bertrand, G. An Air-Stable Oxyallyl Radical Cation. *Angew. Chem., Int. Ed.* **2013**, *52*, 7014−7017. (c) Mahoney, J. K.; Martin, D.; Moore, C. E.; Rheingold, A. L.; Bertrand, G. Bottleable (Amino)(Carboxy) Radicals Derived from Cyclic (Alkyl)(Amino) Carbenes. *J. Am. Chem. Soc.* **2013**, *135*, 18766−18769. (d) Kretschmer, R.; Ruiz, D. A.; Moore, C. E.; Rheingold, A. L.; Bertrand, G. One-, Two-, and Three-Electron Reduction of a Cyclic Alkyl-(Amino)Carbene-Sbcl$_3$ Adduct. *Angew. Chem., Int. Ed.* **2014**, *53*, 8176−8179. (e) Li, Y.; Mondal, K. C.; Samuel, P. P.; Zhu, H.; Orben, C. M.; Panneerselvam, S.; Dittrich, B.; Schwederski, B.; Kaim, W.; Mondal, W. T.; Koley, D.; Roesky, H. W. C$_4$ Cumulene and the Corresponding Air-Stable Radical Cation and Dication. *Angew. Chem., Int. Ed.* **2014**, *53*, 4168−4172. (f) Roy, S.; Stuckl, A. C.; Demeshko, S.; Dittrich, B.; Meyer, J.; Maity, B.; Koley, D.; Schwederski, B.; Kaim, W.; Roesky, H. W. Stable Radicals from Commonly Used Precursors Trichlorosilane and Diphenylchlorophosphine. *J. Am. Chem. Soc.* **2015**, *137*, 4670−4673. (g) Roy, S.; Mondal, K. C.; Roesky, H. W. Cyclic Alkyl(Amino) Carbene Stabilized Complexes with Low Coordinate Metals of Enduring Nature. *Acc. Chem. Res.* **2016**, *49*, 357−369. (h) Munz, D.; Chu, J.; Melaimi, M.; Bertrand, G. Nhc-Caac Heterodimers with Three Stable Oxidation States. *Angew. Chem., Int. Ed.* **2016**, *55*, 12886−12890. (i) Mahoney, J. K.; Martin, D.; Thomas, F.; Moore, C. E.; Rheingold, A. L.; Bertrand, G. Air-Persistent Monomeric (Amino)(Carboxy) Radicals Derived from Cyclic (Alkyl)(Amino) Carbenes. *J. Am. Chem. Soc.* **2015**, *137*, 7519−7525. (j) Hansmann, M. M.; Melaimi, M.; Munz, D.; Bertrand, G. A Modular Approach to Kekulé Diradicaloids Derived from Cyclic (Alkyl)(Amino)Carbenes. *J. Am. Chem. Soc.* **2018**, *140*, 2546−2554.

(11) (a) Weinstein, C. M.; Junor, G. P.; Tolentino, D. R.; Jazzar, R.; Melaimi, M.; Bertrand, G. Highly Ambiphilic Room Temperature Stable Six-Membered Cyclic (Alkyl)(Amino)Carbenes. *J. Am. Chem. Soc.* **2018**, *140*, 9255−9260. (b) Romero, E. A.; Zhao, T. X.; Nakano, R.; Hu, X.; Wu, Y.; Jazzar, R.; Bertrand, G. Tandem Copper Hydride−Lewis Pair Catalysed Reduction of Carbon Dioxide into Formate with Dihydrogen. *Nat. Catal.* **2018**, *1*, 743−747. (c) Nascimento, D. L.; Fogg, D. E. Origin of the Breakthrough Productivity of Ruthenium-Cyclic Alkyl Amino Carbene Catalysts in Olefin Metathesis. *J. Am. Chem. Soc.* **2019**, *141*, 19236−19240. (d) Yazdani, S.; Junor, G. P.; Peltier, J. L.; Gembicky, M.; Jazzar, R.; Grotjahn, D. B.; Bertrand, G. Influence of Carbene and Phosphine Ligands on the Catalytic Activity of Gold Complexes in the Hydroamination and Hydrohydrazination of Alkynes. *ACS Catal.* **2020**, *10*, 5190−5201. (e) Jazzar, R.; Soleilhavoup, M.; Bertrand, G. Cyclic(Alkyl)-and(Aryl)-(Amino)Carbene Coinage Metal Complexes and Their Applications. *Chem. Rev.* **2020**, *120*, 4141−4168. (f) Morvan, J.; Mauduit, M.; Bertrand, G.; Jazzar, R. Cyclic (Alkyl)(Amino)Carbenes (CAACs) in Ruthenium Olefin Metathesis. *ACS Catal.* **2021**, *11*, 1714−1748.

(12) Oldroyd, N. L.; Chitnis, S. S.; Annibale, V. T.; Arz, M. I.; Sparkes, H. A.; Manners, I. Metal-Free Dehydropolymerisation of Phosphine-Boranes Using Cyclic (Alkyl)(Amino)Carbenes as Hydrogen Acceptors. *Nat. Commun.* **2019**, *10*, 1370.

(13) Xu, S.; Manna, K.; Ellern, A.; Sadow, A. D. Mixed N-Heterocyclic Carbene−Bis(Oxazolinyl)Borato Rhodium and Iridium Complexes in Photochemical and Thermal Oxidative Addition Reactions. *Organometallics* **2014**, *33*, 6840−6860.

(14) Tran, B. L.; Fulton, J. L.; Linehan, J. C.; Lercher, J. A.; Bullock, R. M. Rh(CAAC)-Catalyzed Arene Hydrogenation: Evidence for Nanocatalysis and Sterically Controlled Site-Selective Hydrogenation. *ACS Catal.* **2018**, *8*, 8441−8449.

(15) Resendiz-Lara, D. A.; Whittell, G. R.; Leitao, E. M.; Manners, I. Catalytic Synthesis, Characterization, and Properties of Polyaminoborane Homopolymers and Random Copolymers. *Macromolecules* **2019**, *52*, 7052−7064.

(16) Sonnenberg, J. F.; Morris, R. H. Evidence for Iron Nanoparticles Catalyzing the Rapid Dehydrogenation of Ammonia-Borane. *ACS Catal.* **2013**, *3*, 1092−1102.

(17) Li, Y.; Zhang, X.; Peng, Z.; Liu, P.; Zheng, X. Highly Efficient Hydrolysis of Ammonia Borane Using Ultrafine Bimetallic Rupd Nanoalloys Encapsulated in Porous G-C$_3$N$_4$. *Fuel* **2020**, *277*, 118243.

(18) Hou, C.; Li, Q.; Wang, C.; Peng, C.; Chen, Q.; Ye, H.; Fu, W.; Che, C.; López, N.; Chen, Y. Ternary Ni−Co−P Nanoparticles as Noble-Metal-Free Catalysts to Boost the Hydrolytic Dehydrogenation of Ammonia-Borane. *Energy Environ. Sci.* **2017**, *10*, 1770−1776.

(19) (a) Baker, R. T.; Ovenall, D. W.; Calabrese, J. C.; Westcott, S. A.; Taylor, N. J.; Williams, I. D.; Marder, T. B. Boryliridium and Boraethyliridium Complexes Fac-[IrH$_2$(PMe$_3$)$_3$(BRR′)] and Fac-[IrH(PMe$_3$)$_3$(K^2-CH$_2$BHRR′)]. *J. Am. Chem. Soc.* **1990**, *112*, 9399−9400. (b) Sewell, L. J.; Lloyd-Jones, G. C.; Weller, A. S. Development of a Generic Mechanism for the Dehydrocoupling of Amine-Boranes: A Stoichiometric, Catalytic, and Kinetic Study of H$_3$B.NMe$_2$H Using the [Rh(PCy$_3$)$_2$]$^+$ Fragment. *J. Am. Chem. Soc.* **2012**, *134*, 3598−3610.

(20) Zimmerman, P. M.; Paul, A.; Zhang, Z.; Musgrave, C. B. The Role of Free N-Heterocyclic Carbene (NHC) in the Catalytic Dehydrogenation of Ammonia-Borane in the Nickel Nhc System. *Angew. Chem., Int. Ed.* **2009**, *48*, 2201−2205.

(21) Stevens, C. J.; Dallanegra, R.; Chaplin, A. B.; Weller, A. S.; Macgregor, S. A.; Ward, B.; McKay, D.; Alcaraz, G.; SaboEtienne, S. [Ir(PCy$_3$)$_2$(H)$_2$(H$_2$B-NMe$_2$)]$^+$ as a Latent Source of Aminoborane: Probing the Role of Metal in the Dehydrocoupling of H$_3$B Center Dot Nme$_2$h and Retrodimerisation of [H$_2$BNMe$_2$]$_2$. *Chem. - Eur. J.* **2011**, *17*, 3011−3020.

(22) (a) Wang, W.; Tang, H.; Lu, W.; Li, Y.; Bao, M.; Himeda, Y. Mechanistic Insights into the Catalytic Hydrolysis of Ammonia Borane with Proton-Responsive Iridium Complexes: An Experimental and Theoretical Study. *ChemCatChem* **2017**, *9*, 3191−3196. (b) Li, Y.; Hu, M.; Wang, J.; Wang, W. Dft Studies on the Ru-Catalyzed Hydrolysis of Ammonia Borane. *J. Organomet. Chem.* **2019**, *899*, 120913.

(23) Romanov, A. S.; Bochmann, M. Gold(I) and Gold(III) Complexes of Cyclic (Alkyl)(Amino)Carbenes. *Organometallics* **2015**, *34*, 2439−2454.

(24) Maier, T. M.; Sandl, S.; Shenderovich, I. G.; Jacobi von Wangelin, A.; Weigand, J. J.; Wolf, R. Amine-Borane Dehydrogenation and Transfer Hydrogenationcatalyzed by a-Diimine Cobaltates. *Chem. - Eur. J.* **2019**, *25*, 238−245.

(25) Guo, K.; Li, H.; Yu, Z. Size-Dependent Catalytic Activity of Monodispersed Nickel Nanoparticles for the Hydrolytic Dehydrogenation of Ammonia Borane. *ACS Appl. Mater. Interfaces* **2018**, *10*, 517−525.